ESTIMATING THE PERMEABILITY OF A POROUS CERAMIC TILE

Abul Borkot Md Rafiqul Hasan[1], Krishna M Pillai[2], Parham Mobadersani[2], Filip Zemajtis[2], and Konstantin Sobolev[2]

[1]Affiliation not available
[2]College of Engineering and Applied Sciences, University of Wisconsin Milwaukee

February 15, 2024

ESTIMATING THE PERMEABILITY OF A POROUS CERAMIC TILE

[1]ABUL BORKOT MD RAFIQUL HASAN, [2]KRISHNA M. PILLAI, [3]PARHAM MOBADERSANI,
[4]FILIP ZEMAJTIS, [5]KONSTANTIN SOBOLEV

College of Engineering and Applied Sciences, University of Wisconsin Milwaukee
E-mail: [1]arhasan@uwm.edu, [2]krishna@uwm.edu, [3]mobader2@uwm.edu, [4]zemajtis@uwm.edu, [5]sobolev@uwm.edu

Abstract - Porous ceramics are widely used for water filtering, improving heat transfer, supporting catalysts, vaporizing liquids, etc. Residential tiles used for water sealing are made from ceramic as well. Moisture infusion analysis based on Richard's equation is necessary to improve tile quality, and this analysis depends heavily on estimating the tile permeability. The current research demonstrates three techniques for calculating ceramic-tile permeability. The first technique is a theoretical model that requires information about the material's effective diameter and porosity that was obtained via scanning electron microscopy (SEM). The second suggested technique is known as mercury intrusion porosimetry (MIP). The pore size, density, pore volume, and porosity of the ceramic tiles, among other characteristics, are evaluated using mercury in this procedure. The experiment's pressure was varied from 0.1 to 60000 psi. These criteria were used to determine the tile's permeability. The last strategy addressed in this research is the falling-head permeameter (FHP) approach. This procedure involves inserting the specimen into a sealed transparent rectangular conduit. Water is then allowed to pass through it. The rate at which the water level in the duct recedes over time is associated with permeability. All the approaches yield permeability values that are in the same order-of-magnitude of 10^{-16} m^2.

Keywords - Permeability, Porous Media, Richard's equation, Ceramic tile, Saturation, Falling-head Permeameter, Mercury Intrusion Porosimetry

I. INTRODUCTION

Porous ceramics are widely used in different areas including their use as liquid and gas filters, residential tiles, liquid transport medium in Loop Heat Pipes (LHP), supports for catalysts,wicks in air freshening devices, etc. [1, 2]. Permeability is an essential property of porous media for predicting fluid velocity in them. The ability to predict permeability in rock samples is useful in petroleum engineering, environmental science, hydrogeology, and other fields. Numerous studies have tried to establish a link between permeability and other easily computed parameters such as porosity and specific surface area, but these correlations have often proved inaccurate in consolidated porous media such as ceramic tiles since their permeability is dependent on detailed microstructure of porous materials [3]. In addition, there is no explicit function for permeability of ceramic that may correlate permeability with particle diameter and porosity, therefore allow one to get a decent estimate easily. Different techniques for determining the permeability of various materials may be found in the scientific literature. All approaches may be categorized into the following three groups: a) Theoretical methods, b) Experimental methods, and c) Numerical methods. There are a variety of permeability expressions in theoretical models. Further classifications include empirical models, deterministic models based on Stokes flow, network models, statistical models, and flow-around-submerged-object models, among others [4]. Most of the theoretical models include an expression composed of the square of the effective diameter and a function of the porosity [5-8]

Literature has a number of experimental techniques for measuring permeability. Constant pressure 1-D flow technique, constant flow rate 1-D flow method, radial flow method (point injection in 2D, line injection in 3D), etc. [4]. A comparison study between falling head and constant head can be found in the literature of Sandoval et.al.[9]. They studied falling head and constant head method for the determination of the permeability and came up with some correlations. Permeability estimations using numerical approaches are also available in the published literature. In their research, Zarandiet al.[5]presented one such approach. They first developed unit cells by randomly distributing parallel fibers in a confined space using the software GeoDict, and then employed two techniques based on the Stokes-flow based physics to estimate numerical permeability. First, they turned to the commercial software Fluent to estimate pressure drop across the unit cell for a specified creeping flow. In their second technique, they relied on Whitaker's closure formulation, which is based on the proof of Darcy's law (the law used for modeling flows in porous media) using the volume averaging method for flows in porous medium. COMSOL was used to solve the closure equations. Both the techniques achieved fairly good comparison with experimentally determined permeability[5]. Mostaghimiet al. provide one of the few alternative numerical methods available for calculating Stokes flow directly on binarized 3D images (obtained through micro-CT imaging) [10]. Permeability measurements of auncoated residential tile using MIP (Mercury Intrusion Porosimetry) and FHP(falling-head permeameter) techniques have not been explored earlier, as shown by the results of the aforementioned literature review and the authors'

previous study. In addition, there is no known explicit function that correlates permeability of ceramic with porosity and particle diameter. Therefore, in the current work, these experimental methodologies are employed to assess the permeability of ceramic tile and compare the measured values to some theoretical models.
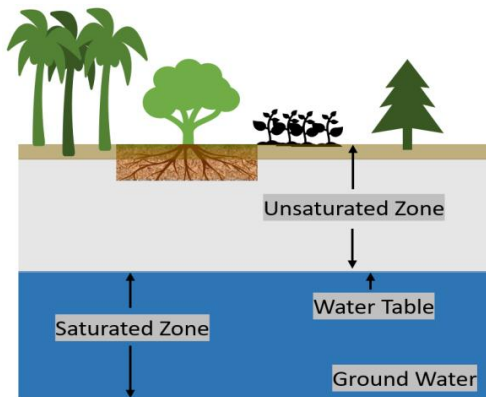
II. BACKGROUND

Understanding how liquid flows through a porous substance is essential for hydrology, petrology, and other geological fields. Similarly, the distribution of water in soil is crucial. To facilitate comprehension, Figure 1.a depicts distinct zones depending on soil moisture content. Dry ceramic surfaces are regarded as being in the unsaturated zone for this study. Water droplets are discharged from a source and land on the ceramic surface. When water comes into contact with ceramic, the area immediately underneath it is known as the saturated zone (Figure 1.b). By solving the following Richards equation, one may determine the distribution of water saturation as it seeps inside under capillary action.

$$\epsilon \frac{\partial S}{\partial t} = \nabla \cdot k_r \frac{K}{\mu} \left(-\frac{d\langle p_C \rangle}{dS} \right) \nabla S \qquad (1)$$
$$+ \frac{K\rho g}{\mu} \left(\frac{dk_r}{dS} \right) \frac{\partial S}{\partial z}$$
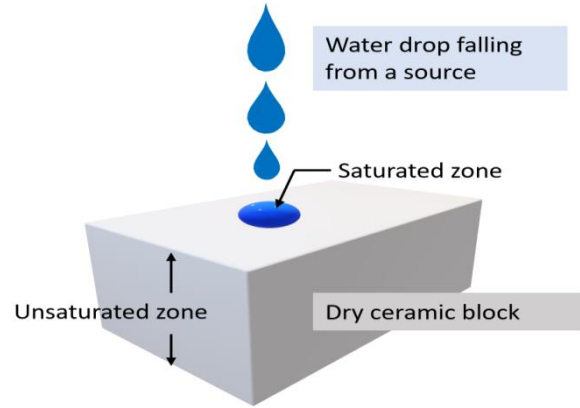
This equation, after including suitable saturation-dependent models for relative permeability and capillary pressure, can be modified further for the ceramic tile as

$$\epsilon \frac{\partial S}{\partial t} = \nabla \cdot \frac{0.04\,K}{\mu} \frac{S^{1.75}}{1-S} \nabla S \qquad (2)$$
$$+ \frac{K\rho g}{\mu} 3S^2 \frac{\partial S}{\partial z}$$

Now, the time-dependent water saturation in the ceramic tile may be predicted by numerically solving this equation. However, the permeability (K) value is needed for this determination. Therefore, the purpose of the current research is to determine permeability using two distinct approaches and compare the findings with predictions of theoretical models.

(a)

(b)

Figure 1: Different zones on the basis of water saturation - a) Soil, b) Reference Ceramic Tile

III. THEORETICAL MODEL

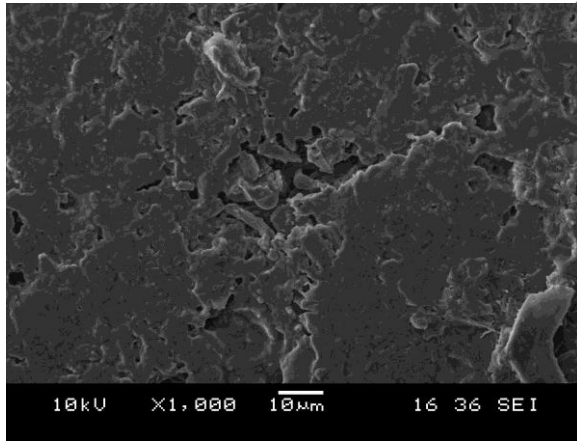Among theoretical models, several expressions for permeability exist. Most theoretical models are of the form

$$K = D_e{}^2 F(\varepsilon) \qquad (3)$$

where D_e is the effective diameter and ε is the porosity. This function of porosity $F(\varepsilon)$ can be estimated for several models: Kezeny-Carman [3], Davies [8], Chen[7], Tomadakis and Robertson [6]. The functions for different model are listed in Table 1.
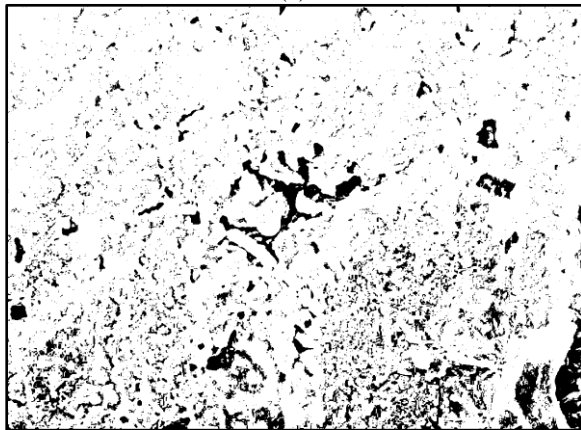
Model	$F(\varepsilon)$	
Kozeny - Carman	$\dfrac{\varepsilon^3}{180\,(1-\varepsilon)^2}$	(4)
Chen	$0.129\,\dfrac{\varepsilon}{(1-\varepsilon)} \ln \dfrac{0.64}{(1-\varepsilon)^2}$	(5)
Tomadakis - Robertson	$\dfrac{\varepsilon}{8 \ln^2 \varepsilon} \dfrac{(\varepsilon-0.11)^{2.785}}{0.912[(1.785)\,\varepsilon - 0.11]^2}$	(6)
Davies	$\dfrac{1}{64\,(1-\varepsilon)^{1.5}[1+56(1-\varepsilon)^3]}$	(7)

Table 1: Porosity function for different model

The porosity of the material was determined in this case using a scanning electron microscope (SEM)(Figure 2.a).The sample was coated with gold for about one minute using a Vacuum Desk coater. Then, the micrograph was obtained. After that, the micrograph was imported to an open-source software Image J. Using the software, first the threshold of the image was adjusted by the mean method with red color. Then it was converted into a binarized image and the color was inverted, final binarized picture is depicted in Figure 2.b.The image was then analyzed using Image J. After the analysis, a porosity of 0.27 and effective diameter of 696.088 nm, which is the average pore diameter for this case, was calculated.

Estimating the Permeability of A Porous Ceramic Tile

(a)

(b)

Figure 2: a) Micrograph of the sample obtained by SEM, b) Corresponding transformed binary picture

Model	Permeability, K (m^2)
Kozeny - Carman	1.09×10^{-16}
Chen	1.36×10^{-14}
Tomadakis - Robertson	1.14×10^{-16}
Davies	8.15×10^{-16}

Table 2: Value of Permeability obtained from different theoretical models

IV. MERCURY INTRUSION POROSIMETRY METHOD

MIP is the second method used for determining the sample material's permeability. Due to its non-wetting property, mercury is the working fluid for this test (described in Table 1). Since mercury does not wet most substances and cannot enter pores by capillary action, it must be forced into pores by external pressure. Mercury can be pushed into large macropores with little pressure, while considerably more pressure is necessary to drive it into minute holes. According to the Washburn equation, the equilibrium pressure is inversely proportional to the pore size.[11]:

$$D_p = -\frac{4\,\gamma\,\cos\theta}{P} \qquad (8)$$

Here, D_P is the pore diameter, γ denotes the surface tension, θ is the contact angle of mercury, and P is the applied pressure.

Property	Value
Adv. Contact Angle, θ	130 degrees
Rec. Contact Angle, θ	130 degrees
Surface Tension, γ	4.65×10^{-1} N/m
Density, ρ	13533.5 Kg/m^3

Table 3: Properties of mercury for the experiment

Mercury porosimetry requires the progressive introduction of mercury into a porous material under controlled circumstances. Using the Washburn equation, the experimental setup calculates volume and size distributions using pressure versus intrusion data. This information is essential for determining the permeability. Katz and Thompson's model serves as the MIP's foundation for determining permeability. [12]. The relation can be expressed as:

$$K = c\,l_c^2\,\frac{\sigma}{\sigma_0} \qquad (9)$$

Here, c is permeability constant in the order of 1/226. l_c is the characteristics length which will be discussed later. σ/σ_0 is the conductivity formation factor.

After repeating the experiment at various pressures ranging from 0.1 psia to 60000 psia, Figures 3 and 4 exhibit the intrusion volume in relation to the injection pressure. The experimentally determined threshold pressure (P_t) is 151.41 psi. At the threshold pressure, the intrusion volume versus pressure curve is at its steepest. This pressure is necessary to identify the length's properties, l_c. Now, based on the Washburn equation:

$$l_c = -\frac{4\,\gamma\,\cos\theta}{P_t} \qquad (10)$$
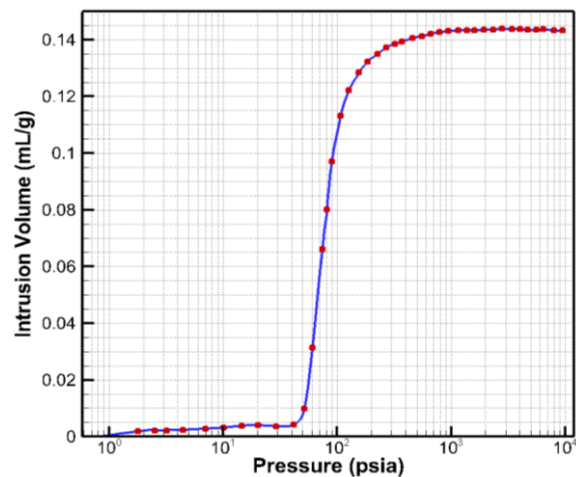

Figure 3: Intrusion volume as a function of pressure
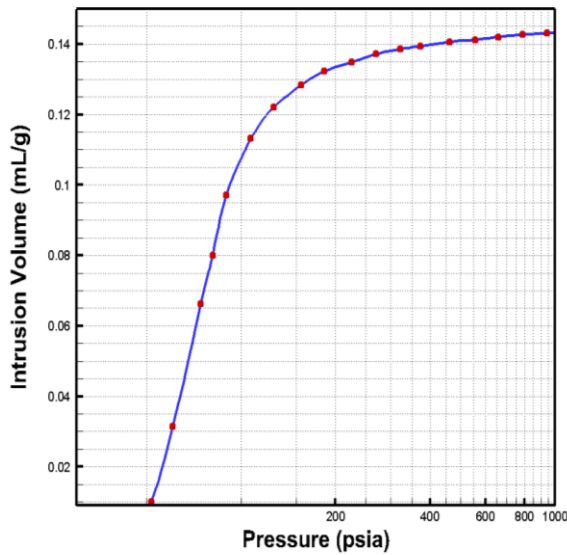
Figure 4: Intrusion volume as a function of pressure subtracting off the surface mercury volume

Now, conductivity formation can be calculated by [13]:

$$\frac{\sigma}{\sigma_0} = \frac{l_{max}^e}{l_c} \, \varepsilon \, S(l_{max}^e) \qquad (11)$$

The highest length at which conductivity occurs is denoted here by l_{max}^e. The $I_v \times D_p^3$ vs D_p curve provides the necessary information for this calculation. I_v stands for the volume of the intrusion. Saturation as a function of l_{max}^e, $S(l_{max}^e)$ is calculated by interpolating the Specific I_v vs. D_P curve at l_{max}^e and dividing by the total specific intrusion volume I_{tv}. ε in the equation is the porosity of the material.

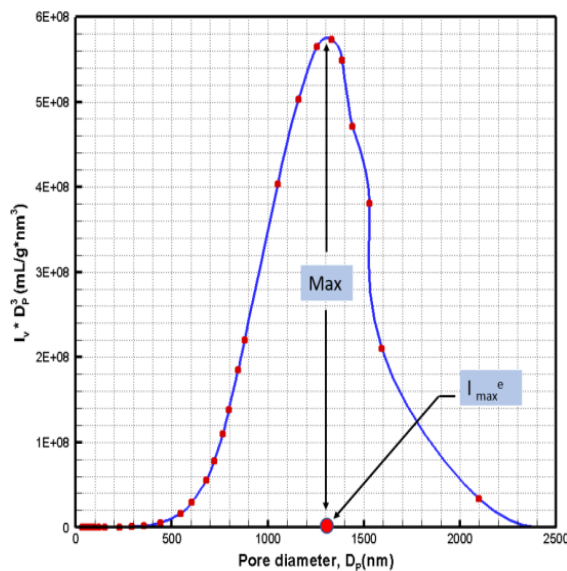**Figure 5: Optimum path for conductivity. Electrical conductance function ($I_v \times D_P^3$) vs. pore diameter which occurs at $l_c = l_{max}^e$**

Calculation parameters	Value
Threshold pressure, P_t	151.41 psia
Characteristic length, l_c	1194.5 nm
Length for maximum conductance, l_{max}^e	1331.87 nm
Porosity, ε	0.36
Permeability constant, c	0.00442
Saturation, $S(l_{max}^e)$	0.1531
Permeability, K	3.86×10^{-16} m^2

Table 4: List of the parameters used in the MIPcomputations

V. FALLING HEAD PERMEABILITY METHOD

The third method used in present study for the determination of permeability is the Falling-Head Permeameter (FHP) method. A schematic of the in-house developed permeameter used in this experiment is depicted in Figure 7. First, the sample is covered with aluminum foil to protect the surfaces from being covered by other materials. Then, a portion of the duct is sliced from the main duct with thickness close to the tile. After that, the ends of the duct are rubbed on a sand paper for surface finish.The sample is positioned inside the sliced portion of the duct, and the gap between the sample and duct wall is sealed from all sides. Finally, the prepared part is joinedto the end of the main duct. Figure. 7 illustrates the experimental setup for permeability measurement by the falling-head method. After the set-upis ready, the water is poured into the duct. Water's starting height (h_1) was noted at time t=0. The water starts penetrating the sample. As water penetrates through a sample, the water level at a falling-head permeameter's input falls over time. Due to the continual lowering of the intake head, which signifies a drop in the input pressure driving the flow, the Darcy velocity inside the porous sample falls. The ultimate height (h_2) is noted after time t. Now, the permeability may be calculated using the relationship shown below:

$$K = \frac{\mu \, a \, L}{\rho \, g \, A \, t} \ln \frac{h_1}{h_2} \qquad (12)$$

Here, a, A are the cross-section of the duct and sample respectively, L is the length of the sample, and t denotes the elapsed time.

Calculation parameter	Value
Density of water (at 22°C), ρ	997.77 kg/m^3
Viscosity of water (at 22°C), μ	10^{-3} Pa.s
Acceleration due to gravity, g	9.81 m/s^2
Duct Cross- sectional area, a	1.69×10^{-4} m^2
Tile Cross- sectional area, A	7.29×10^{-5} m^2

Table 5: List of parameter values used for FHP computations

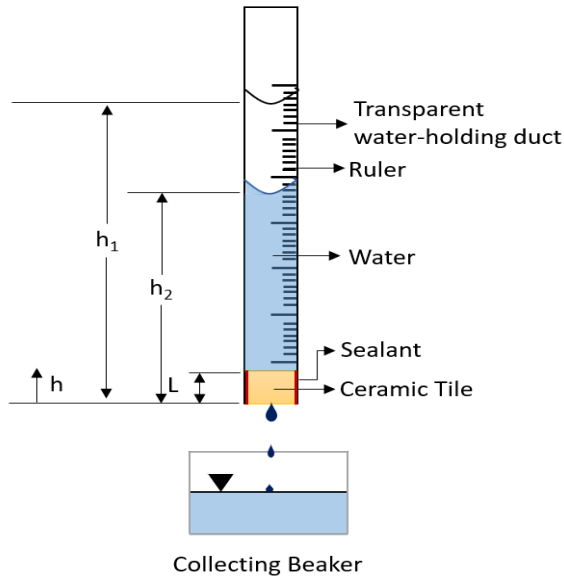Estimating the Permeability of A Porous Ceramic Tile

Figure 6: Schematic of the falling head permeameter (FHP)

Each of six experiments took two days because of the slow seepage of water through the tile. Table 3 lists the calculation parameters used in the present experiment. The scatter in the permeability was determined using the 95% confidence interval from six separate experiments.The final K value was computed to be $(6.09 \pm 1.25) \times 10^{-16}$ m^2.
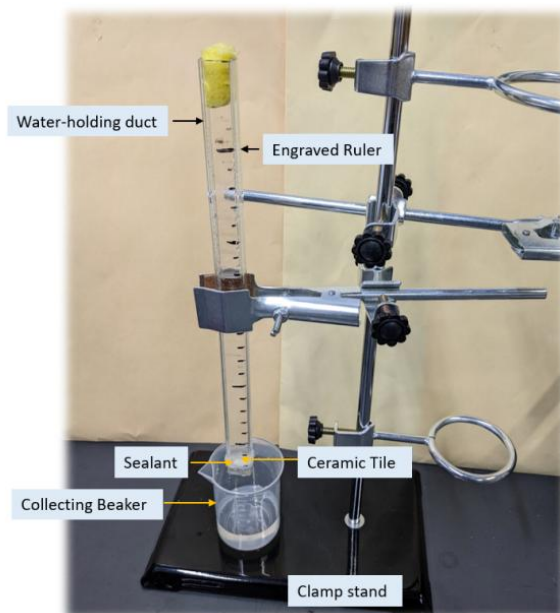

Figure 7: The experimental setup built in-house for permeability measurement by the falling head permeameter principle

VI. CONCLUSION

The permeability determined by each of the three outlined approaches is of the same order of magnitude (x 10^{-16} m^2). Of the four theoretical models considered, only the Chen modelis deviant and predicts permeability on the order of 10^{-14} m^2. The

difference between Kozeny- Carman and Tomadakis - Robertson is only around 4%. Again, the permeability determined by the Davies model is comparable to that determined by the falling-head permeameter. Consequently, the permeability of this order of magnitude can be used to solve Richard's equation to get the saturation distribution within the ceramic tile.

ACKNOWLEDGEMENT

NOMENCLATURE

Symbol	Definition	Unit
a	Cross-sectional Area of duct	m^2
c	Permeability constant	
g	Acceleration due to gravity	m/s^2
h$_1$	Initial height	m
h$_2$	Final height	m
g	Acceleration due to gravity	m/s^2
h$_1$	Initial height	m
h$_2$	Final height	m
k$_r$	Relative permeability	
l$_c$	Characteristics length	m
l$_{max}$^{e}	Length for maximum conductance	m
p$_c$	Capillaty pressure	Pa
A	Cross-sectional Area of sample	m^2
D$_b$	Solid particle Diameter	m
D$_p$	Pore Diameter	m
I$_{tv}$	Total intrusion volume	m^3
I$_v$	Intrusion volume	m^3
K	Permeability	m^2
L	Length of the sample	m
P$_t$	Threshold pressure	Pa
S	Saturation	
Greek		
γ	Surface Tension	N/m
ε	Porosity	
θ	Contact angle	Degree
μ	Viscosity	Pa.s
ρ	Density	Kg/m^3

REFERENCE

[1] U. Werr, "Porous ceramics manufacture–properties–applications," in CFI-Ceramic Forum International, 2014, vol. 8.

[2] P. H. Santos, E. Bazzo, S. Becker, R. Kulenovic, and R. Mertz, "Development of LHPs with ceramic wick," Applied Thermal Engineering, vol. 30, no. 13, pp. 1784-1789, 2010.

[3] J. Bear, Dynamics of fluids in porous media. Courier Corporation, 1988.

[4] R. Masoodi and K. M. Pillai, Wicking in porous materials: traditional and modern modeling approaches. CRC Press, 2012.

[5] M. A. F. Zarandi, S. Arroyo, and K. M. Pillai, "Longitudinal and transverse flows in fiber tows: Evaluation of theoretical permeability models through numerical predictions and experimental measurements," Composites Part A: Applied Science and Manufacturing, vol. 119, pp. 73-87, 2019.

[6] M. M. Tomadakis and T. J. Robertson, "Viscous permeability of random fiber structures: comparison of electrical and diffusional estimates with experimental and analytical results," Journal of Composite Materials, vol. 39, no. 2, pp. 163-188, 2005.

[7] F. Dullien, "Single-phase transport phenomena in porous media," Porous Media: Fluid transport and pore structure, vol. 1, pp. 157-230, 1992.

[8] F. Dullien and H. Brenner, "4-Selected operations involving transport of a single fluid phase through a porous medium," Porous Media, pp. 319-332, 1992.

[9] G. F. B. Sandoval, I. Galobardes, R. S. Teixeira, and B. M. Toralles, "Comparison between the falling head and the constant head permeability tests to assess the permeability coefficient of sustainable Pervious Concretes," Case Studies in Construction Materials, vol. 7, pp. 317-328, 2017/12/01/ 2017.

[10] P. Mostaghimi, M. J. Blunt, and B. Bijeljic, "Computations of Absolute Permeability on Micro-CT Images," Mathematical Geosciences, vol. 45, no. 1, pp. 103-125, 2013/01/01 2013.

[11] E. W. Washburn, "The dynamics of capillary flow," Physical review, vol. 17, no. 3, p. 273, 1921.

[12] Katz and A. Thompson, "Quantitative prediction of permeability in porous rock," Physical review B, vol. 34, no. 11, p. 8179, 1986.

[13] Katz and A. Thompson, "Prediction of rock electrical conductivity from mercury injection measurements," Journal of Geophysical Research: Solid Earth, vol. 92, no. B1, pp. 599-607, 1987.

★ ★ ★